ENGINEERING TRANSACTIONS • *Engng. Trans.* • **45**, 3–4, 419–431, 1997
Polish Academy of Sciences • Institute of Fundamental Technological Research

NUMERICAL MODELLING OF ADIABATIC SHEAR BAND FORMATION IN A TWISTING TEST

A. GLEMA, W. KĄKOL and T. ŁODYGOWSKI (POZNAŃ)

The objective of the paper is the investigation of adiabatic shear band localized fracture phenomenon in a tubular specimen during dynamic loading processes. The fracture occurs as a result of an adiabatic shear band localization attributed to a plastic instability implied by thermal softening during dynamic plastic flow. The formulation of the physical problem is adopted following the paper by T. ŁODYGOWSKI and P. PERZYNA [8]. For regularized elasto-viscoplastic model, the numerical investigation of the three-dimensional dynamic adiabatic deformation in a particular body at nominal strain rates ranging from 10^3 to 10^4 s^{-1} is presented. The attention is focussed on the discussion, which finite element models are acceptable for computational simulation of the real experiments, taking into account both the physical point of view and the computational efficiency. The restrictions in the creation of arbitrary 3-D models are discussed and for the case under consideration, a 2-D shell model is proposed. The results of computations (plastic strains and temperature rise) obtained in the environment of ABAQUS package [1] confirm the laboratory observations with satisfying accuracy.

1. INTRODUCTION

The phenomenon of localization of deformations is observed in a wide range of experiments for the specimens made of brittle as well as ductile materials. The laboratory tests confirm the appearance of relatively narrow zones of intense straining which are usually the precursors of failure. The results of many experiments show the reduction of load carrying capacity together with the increasing localized deformations after the limit load has been obtained. This behaviour is called softening. For this reason some of the materials including metals, soils, concrete and rocks are classified as the so-called softening materials; however, the localization effects depend not only on the material properties but significantly on the boundary and initial conditions and the shape of the specimens.

The width and the directions of localized zones can not be known *a priori* as material properties but they should appear as a result of the initial boundary value problem (IBVP). The reasons for the softening behaviour of the material can be, for example, the phenomena of porosity nucleation and growth as well as the rise of temperature.

In this approach, a simple mapping of experimental data onto the stress-strain relations provides a negative stiffness in the constitutive model. The significant consequences of this fact discussed on the level of theoretical formulation and numerical analysis were presented by P. PERZYNA [14], T. ŁODYGOWSKI [6, 7] and T. ŁODYGOWSKI and P. PERZYNA [8], and will be not stressed in this presentation. Let us only mention that the softening behaviour leads to ill-posed IBVPs, and for the uniqueness and stability of the solution, the formulation requires regularization. The methods which are used to regularize the system of governing equations (e.g. nonlocal theories, Cosserat continua, the so-called higher order gradient formulations, rate-dependent formulations) and which explicitly or implicitly introduce the so-called length scale parameters, ensure that the type of the operator remains unchanged even in the postcritical range.

Main objective of the paper is the investigation of adiabatic shear bands, and in particular, attention is focussed on modelling the problems that appear in numerical simulation of the twisting test. In the case under consideration, the choice of numerical model plays a significant role in the accuracy of reproducing the results of laboratory tests and, in general, because of the large dimensions of the models, in the possibility of numerical simulation of any results in an acceptable CPU time.

In this formulation we use the rate-dependent (viscoplastic) formulation which allows us to carry out successful analysis also in postcritical plastic states, and which introduces the length scale parameter (regularization parameter) via the relaxation time of mechanical disturbances and the speed of elastic wave propagation. This requires a full dynamic analysis of the process under consideration. The rate-dependent model is physically well-founded, in particular for the high-speed processes in ductile materials.

2. ASSUMPTIONS

The motivation for this numerical study comes from the experiments of K.A. HARTLEY, J. DUFFY and R.H. HAWLEY [4], A. MARCHAND and J. DUFFY [9] and A.M. MERZER [10]. In particular in the first two works, the authors made the macroscopic observations of the shear band localization on the thin-walled steel tubes in the split Hopkinson torsion bar. Different kinds of steel were tested. Main dimensions of the specimen, for which the dynamic deformation in shear was imposed to produce shear bands, are presented in Fig. 1.

The results were obtained for the specimen made of 1018CRS steel for which the nominal rate of shear strain $\dot{\gamma}$ is of the order of $1000\,\mathrm{s}^{-1}$. In the experiment, the changes of temperature and the width of the shear band were measured. It

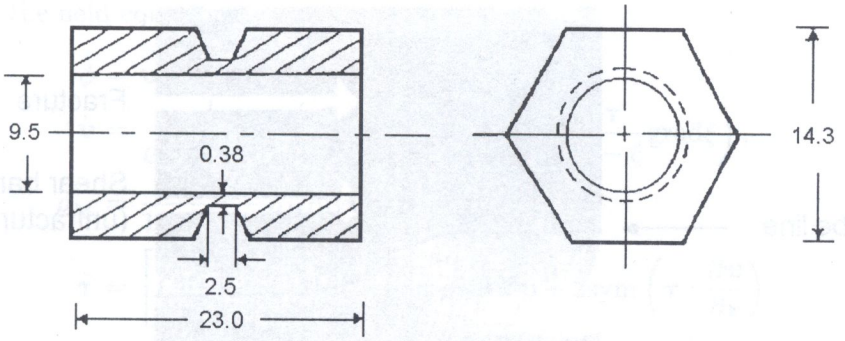

FIG. 1. Details of specimen with hexagonal mounting flanges used in the torsional Kolsky bar experiment (all dimensions are in millimeters), cf. HARTLEY, DUFFY AND HAWLEY (1987), [4].

was found that when the shear band leads to fracture of the tested specimen, the fracture occurrs by a process of void nucleation, growth and coalescence, in the conditions of thermal softening that results from the local temperature rise occurring during the plastic deformation process.

Numerical simulation of the whole range of the experiment should also include the fracture criteria, but they will be omitted in the presentation.

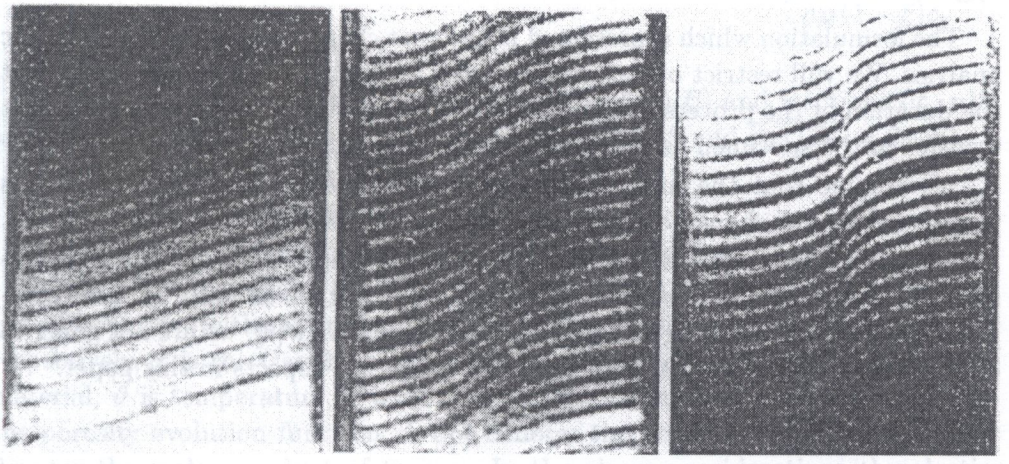

FIG. 2. Grid patterns obtained for HY–100 steel at a nominal strain rate of $1600\,s^{-1}$ [4, 9] for different stages of the process: a) homogeneous deformation, b) inhomogeneous shear strain distribution, c) shear band.

Qualitatively, some experimental results obtained in [4, 9] for HY–100 steel are presented in Fig. 2. The surface of the specimen with shear band and partial fracture is presented in Fig. 3 following the results of J. DUFFY and coworkers [4, 9]. All these figures that describe the experimental results serve as a comparative material with our numerical simulations.

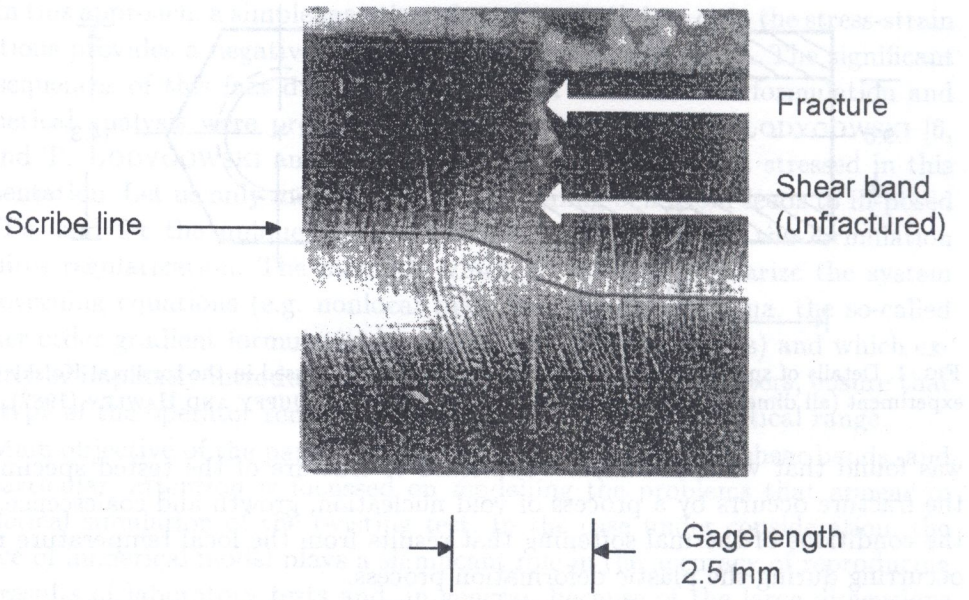

FIG. 3. Specimen surface with a shear band and partial fracture. Nominal strain rate $1600\,s^{-1}$, local shear band $\gamma_{LOC} = 500\%$. [4, 9].

The formulation which is presented in the next chapter requires a full dynamic analysis. We will restrict our attention to the adiabatic processes assuming that the duration of the process of the order of 10^{-4} s allows us to disregard the heat transfer in the specimen as well as the convection and radiation.

We assume that the material of the specimen tested is isotropic and this property does not change during deformations.

Assuming that the formulation of the IBVP satisfies all the conditions necessary to assure the well-posedness [7, 8, 14], what in turn in finite element computations leads to avoiding the spurious mesh sensitivity [6], we are not going to discuss those important mathematical and numerical aspects in this paper.

3. STATEMENT OF THE PROBLEM

The rate-type constitutive structure for an elastic visco-plastic damaged material was discussed in [8]. The formulation introduces the effects of microdamage mechanism and thermomechanical coupling. In the form presented in [8], the adiabatic evolution problem is described as follows.

Find ϕ, $\boldsymbol{\upsilon}$, ϱ_M, $\boldsymbol{\tau}$, ξ and ϑ as functions of time t and space variable $\mathbf{x}$ such that the following conditions are satisfied:

(i) the field equations

$$
\begin{aligned}
\dot{\phi} &= \mathbf{v}, \\
\dot{\mathbf{v}} &= \frac{1}{\varrho_M^0(1-\xi_0)}\left(\frac{\boldsymbol{\tau}}{\varrho_M}\mathrm{grad}\varrho_M + \mathrm{div}\boldsymbol{\tau} - \frac{\boldsymbol{\tau}}{1-\xi}\mathrm{grad}\xi\right), \\
\dot{\varrho}_M &= \frac{\varrho_M}{1-\xi}\Xi - \varrho_M \mathrm{div}\mathbf{v}, \\
\dot{\boldsymbol{\tau}} &= \left[\mathcal{L}^e - \frac{1}{c_p\varrho_{\mathrm{Ref}}}\vartheta\mathcal{L}^{th}\frac{\partial\boldsymbol{\tau}}{\partial\vartheta}\right] : \mathrm{sym}D\mathbf{v} + 2\mathrm{sym}\left(\boldsymbol{\tau} : \frac{\partial\mathbf{v}}{\partial\mathbf{x}}\right) \\
&\quad - \left[\left(\frac{\chi^*}{\varrho_M(1-\xi)c_p}\mathcal{L}^{th}\boldsymbol{\tau} + \mathcal{L}^e + \mathbf{g}\boldsymbol{\tau} + \boldsymbol{\tau}\mathbf{g}\right) : \mathbf{P}\right]\frac{1}{T_m}\left\langle\left(\frac{f}{\kappa}-1\right)^m\right\rangle \\
&\quad - \frac{\chi^{**}\mathcal{L}^{th}}{\varrho_M(1-\xi)c_p}\Xi, \\
\dot{\xi} &= \Xi, \\
\dot{\vartheta} &= \frac{\vartheta}{c_p\varrho_{\mathrm{Ref}}}\frac{\partial\boldsymbol{\tau}}{\partial\vartheta} : \mathrm{sym}D\mathbf{v} + \frac{\chi^*}{\varrho_M(1-\xi)c_p}\boldsymbol{\tau} : \mathbf{P}\frac{1}{T_m}\left\langle\left(\frac{f}{\kappa}-1\right)^m\right\rangle \\
&\quad + \frac{\chi^{**}}{\varrho_M(1-\xi)c_p}\Xi;
\end{aligned}
\tag{3.1}
$$

(ii) the boundary conditions

(a) displacement ϕ is prescribed on a part ∂_ϕ of $\partial\phi(\mathcal{B})$ and tractions $(\boldsymbol{\tau}\cdot\mathbf{n})^a$ are prescribed on part $\partial_{\boldsymbol{\tau}}$ of $\partial\phi(\mathcal{B})$, where $\partial_\phi \cap \partial_{\boldsymbol{\tau}} = 0$ and $\overline{\partial_\phi \cup \partial_{\boldsymbol{\tau}}} = \partial\phi(\mathcal{B})$;

(b) heat flux $\mathbf{q}\cdot\mathbf{n} = 0$ is prescribed on $\partial\phi(\mathcal{B})$;

(iii) the initial conditions

ϕ, $\mathbf{v}$, σ_M, ϑ, ξ and $\boldsymbol{\tau}$ are given at each particle $X \in \mathcal{B}$ at $t = 0$.

In the above equations ϕ is the displacement field, $\mathbf{v}$ is the velocity vector, ϱ_M and ϱ_M^0 denote the actual and reference mass density of the matrix material, respectively, $\boldsymbol{\tau}$ is the Cauchy stress tensor, ξ_0 describes the initial porosity of a material, ϑ is temperature, $D\mathbf{v}$ denotes the spatial velocity gradient, and Ξ is the porosity evolution function. A dot denotes the time derivative, and colon : denotes the scalar product of tensors. In the above considerations the elastic visco-plastic model of the material [12, 13] was assumed so that

$$
\Lambda = \frac{1}{T_m}\langle\Phi(f-\kappa)\rangle,
\tag{3.2}
$$

where T_m is the relaxation time of mechanical perturbances, and Φ is a postulated overstress visco-plastic function

$$
\Phi(f-\kappa) = \left(\frac{f}{\kappa}-1\right)^m, \qquad \text{where} \quad m = 1,3,5,\ldots\,.
\tag{3.3}
$$

The plastic potential function for the material was assumed in the form dependent on the second invariant of deviatoric stress as well as on the hydrostatic state J_1

$$f = J_2 + n\xi {J_1}^2. \tag{3.4}$$

Continuing the explanation of the symbols used let us observe that $\mathcal{L}^e$ and $\mathcal{L}^{th}$ are the mechanical and thermal operators, Ξ is the function which describes the process of nucleation and growth of voids, χ^* and χ^{**} are the irreversibility coefficients and

$$\mathbf{P} = \frac{1}{2\sqrt{J_2}} \frac{\partial f}{\partial \boldsymbol{\tau}}.$$

In our numerical considerations we will omit the terms that describe the influence of porosity. We arrive then at a simplified system of equations if we assume the porosity $\xi = 0$, neglect the porosity evolution function Ξ and the irreversibility coefficients $\chi^* = 0$ and $\chi^{**} = 0$.

4. Numerical models

In the original experiment, the tested specimens were produced in the form of thin-walled tubes with integral hexagonal flanges for gripping.

The following chapter is devoted to the discussion of the problem of proper selection of the finite element model which would be numerically efficient and lead to the results complying with experimental data. The remarks on how to model the boundary and initial conditions is then the natural part of the modelling problems.

For the rate-dependent plasticity model used, the plastic part of the rate of deformation for the states $f \geq \kappa$ is expressed by

$$\mathbf{d}^p = \frac{1}{T_m} \left(\frac{f}{\kappa} - 1 \right)^m, \qquad \text{where} \quad m = 1, 3, 5, \ldots, \tag{4.1}$$

and the adiabatic rise of temperature due to pure mechanical dissipation is found as a part of it

$$\varrho c_p(\vartheta)\dot{\vartheta} = \eta r(\boldsymbol{\tau}, \mathbf{d}), \tag{4.2}$$

where $c_p(\vartheta)$ is the heat capacity, $\mathbf{d}$ denotes the deformation velocity, $r(\boldsymbol{\tau}, \mathbf{d})$ is the plastic rate of dissipation and η is the percentage of plastic work converted into heat.

The computational model was created and analysed in the environment of a general purpose finite element program ABAQUS with the necessary modifications in constitutive behaviour.

In the laboratory tests [4, 9], both the width of the shear band (plastic strain localization zone) and the temperature changes have been found. To reproduce in the numerical simulations the high gradients of plastic strains and temperatures, it is necessary to use relatively dense meshes in the area of intensive straining; see e.g. B. LORET and J.H. PREVOST [5]. For this purpose we have to use fine meshes, at least in vicinity of the expected zones of localized strains. In the experiment, the measured values of the shear bands widths were of the order of $0.2 - 0.3$ mm. This result significantly reduces the smallest dimension of the FE mesh of the model.

4.1. Model simplification

In the recent years H.M. ZBIB and J.S. JUBRAN [15] have numerically investigated a three-dimensional problem involving the development of shear bands in a steel bar pulled in tension. 4340 steel thin tube twisted in a split Hopkinson bar at different nominal strain rates (1000 to $25\,000\,\mathrm{s}^{-1}$) was computed by R.C. BATRA and X. ZHANG [2]. In both of the cited papers the 3-D 8-node brick elements were used.

When modelling the problem under consideration, we started with the model of the whole specimen including the tube and the flanges. The so-called geometrical model, prepared by using PATRAN Pre and Postprocessor, which shows only the view of the specimen or half of it but does not include the finite element mesh, is shown in Fig. 4. We do not present here the FE mesh because the necessary density of the mesh (it should include at least 4 elements along the radial direction of the tube and some hundred elements in the circumferential direction) would destroy the visibility of the model.

For the whole 3-D model, the number of degrees of freedom (DoF) that could reasonably reproduce in numerical analysis the behaviour of the specimen in the interesting domains (shear bands), was of the order of half a million. For such complicated nonlinear computations (large deformations, adiabatic plasticity) which also require many increments including time integration, such large models cannot be acceptable.

Of course, for this model it is natural to define the boundary and initial conditions very close to those which are realized in laboratory tests. It appears that the time necessary to obtain the results even for the most powerful modern computers practically tends to infinity.

There are still very serious limitations in utilizing 3-D model of only half of a tube. If the geometrical model is meshed so that it can give a chance to simulate the real experiment properly, the numerical model has still 79 200 DoF. Figure 5b presents the course mesh which is not dense enough and consists of $24 \times 10 \times 4$

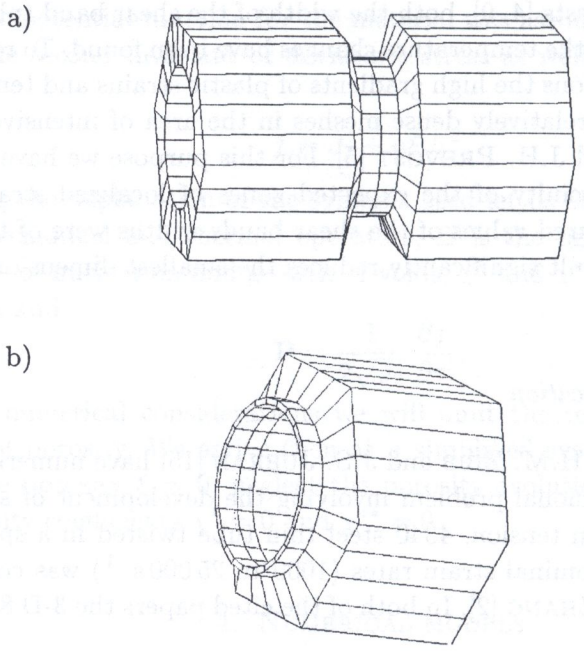

FIG. 4. Geometrical model of the specimen: thin-walled tube and the flanges; a) full model, b) half of the model.

elements. The mesh that could be acceptable has 4 elements in the radial, 240 elements in circumferential, and 10 elements along the axial directions of the tube. Next simplification of the numerical model are the 2-D elements.

It is well known that for a such a complex problem, the only efficient method of time integration of the governing system of dynamic equations is the explicit one [1]. This is, however, conditionally stable but because it does not require the solution of the huge system of equations, it is much faster than the implicit method.

The other very important problems to be solved in the attempt to model the torsional bar using only the thin-walled tube are the initial and boundary conditions. Particularly, to avoid the multiple reflections of waves, one has to replace the interaction of flanges in the experiment by a proper definition of displacements of the edges. It will be done in our numerical computations by adding a mass on the spring which models the elastic deformation of flanges.

Finally, to ensure the efficiency and accuracy, we have decided to use shell elements (4-node with selective reduced integration) with 5 points of integration across the thickness of the element. We model only one half of the tube assuming that the behaviour is symmetric with respect to the central (middle) cross-section. The thin-walled cylinder is then modelled by a shell and consists of

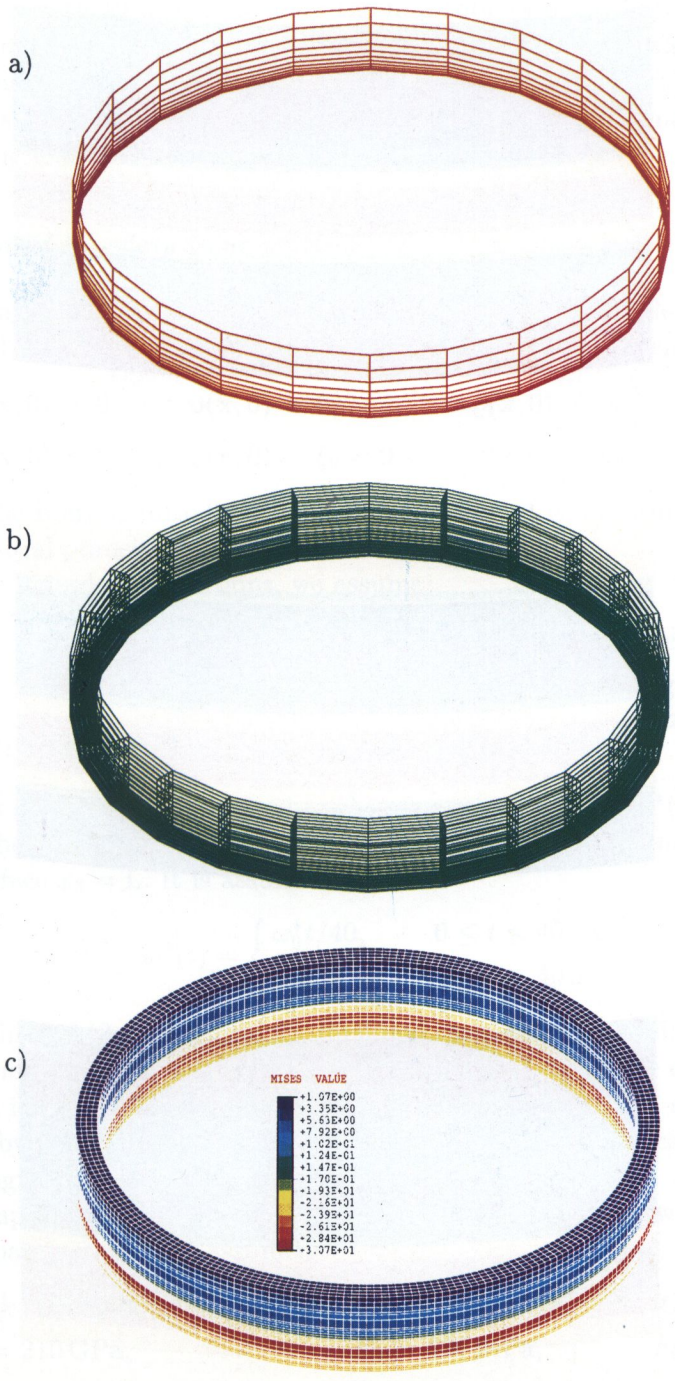

FIG. 5. a) The model of the half-tube with 2-D shell elements. b) The coarse mesh for 3-D model of a half of the tube. c) Distribution of Huber – Mises stresses for 3-D model.

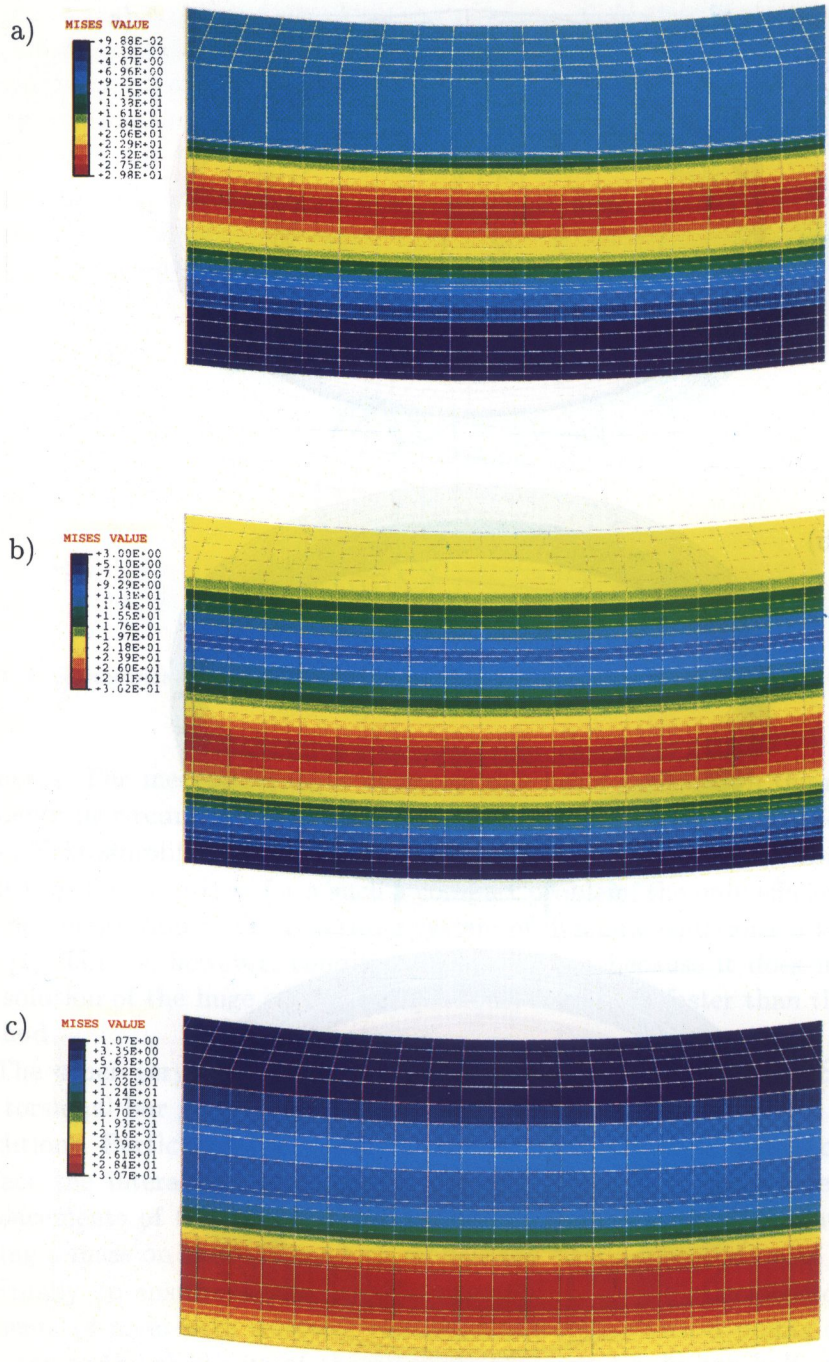

FIG. 6. The sequence of plastic equivalent strains as an effect of wave propagation for a repeated segment a)-c) 2-D model.

24 segments with 10 elements along the half-tube (see Fig. 5a). In the segment, the elements are not equal and their distribution along the depth is such that the mesh is finer close to the internal surface where we can expect a concentration of plastic strains and temperature, and is coarse at the external surface where the twisting load has to be applied.

4.2. Initial boundary value problem

We idealize the initial boundary value problem using the following conditions. The initial conditions for the specimen under analysis are taken in the form

$$
\begin{aligned}
&\phi(\mathbf{x},0) = 0, \qquad \boldsymbol{\upsilon}(\mathbf{x},0) = 0, \qquad \varrho(\mathbf{x},0) = \varrho_{\mathrm{Ref}} = \varrho_M^0(1-\xi_0),\\
&\boldsymbol{\tau}(\mathbf{x},0) = 0, \qquad \xi(\mathbf{x},0) = \xi_0 = 0, \qquad \vartheta(\mathbf{x},0) = \vartheta_0 = \text{constant in } \mathcal{B}.
\end{aligned} \tag{4.3}
$$

That is, the body is initially at rest, is stress-free at a uniform temperature ϑ_0 and the initial porosity at every material point is $\xi_0 = 0$.

For the boundary conditions, we assume

$$
\begin{aligned}
&\boldsymbol{\tau}\cdot\mathbf{n} = 0 \quad \text{on the inner and outer surfaces of the tube,}\\
&\mathbf{q}\cdot\mathbf{n} = 0 \implies \operatorname{grad}\vartheta\cdot\mathbf{n} = 0 \quad \text{on all bounding surfaces,}\\
&\boldsymbol{\upsilon}(x_1,x_2,0,t) = 0, \qquad \boldsymbol{\upsilon}(x_1,x_2,\mathrm{L},t) = \omega^*(t)\left(x_1^2+x_2^2\right)^{1/2}\mathbf{n}^*,
\end{aligned} \tag{4.4}
$$

where $\mathbf{n}$ is a unit outward normal to the respective surfaces, $\omega^*(t)$ is the angular speed of the end cross-section $x_3 = \mathrm{L}$ of the tube, and $\mathbf{n}^*$ is a unit vector tangent to the surface $x_3 = \mathrm{L}$. It is assumed that

$$
\omega^*(t) = \begin{cases} \omega_0^* t/40, & 0 \le t \le 40\,\mu\mathrm{s},\\ \omega_0^*, & t > 40\,\mu\mathrm{s}. \end{cases} \tag{4.5}
$$

The rise time of 40 μs is typical for torsional tests done in a split Hopkinson bar.

To avoid the reflection of waves and to model the influence of the rest of the specimen, it has been assumed that the remaining part of the specimen will be modelled by the additional spring and mass (their characteristics reflect the mass and the rigidity of flanges).

To compare the results with AISI 1018 CRS steel, the following values of the material parameters were assumed:

$$
\begin{aligned}
&\varrho_M = 7860\,\mathrm{kg/m^3}, && c_p = 460\,\mathrm{J/kg\,^\circ C}, && G = 80\,\mathrm{GPa},\\
&K = 210\,\mathrm{GPa}, && \kappa_0 = 237\,\mathrm{MPa}, && \vartheta_0 = 20^\circ\mathrm{C},\\
&m = 5 \ (\text{for } \vartheta = 0^\circ\mathrm{C}), && T_m = 2.5\cdot 10^{-2}\,\mathrm{s} && (\text{for } \vartheta = 0^\circ\mathrm{C}),\\
&m = 4.7 \ (\text{for } \vartheta = 80^\circ\mathrm{C}), && T_m = 1.0\cdot 10^{-2}\,\mathrm{s} && (\text{for } \vartheta = 80^\circ\mathrm{C}).
\end{aligned}
$$

The tube has been twisted at nominal shear strain rates ranging from 10^3 to 10^4 s^{-1}.

For the example considered $\omega^* = 253\,s^{-1}$ has been assumed.

First, in Fig. 5c the distribution of Huber-Mises stresses is presented for a 3-D model. In Fig. 6 the sequence of the same stresses which propagate in time is shown. This confirms the wave character of the phenomena. In fact, the interaction of waves is the only reason which results in a choice of the position and the width of plastic strain localization zones.

Let us now compare qualitatively the evolution of the mesh deformation for a typical segment. In Fig. 7 a sequence of deformed 2-D meshes is presented. At the

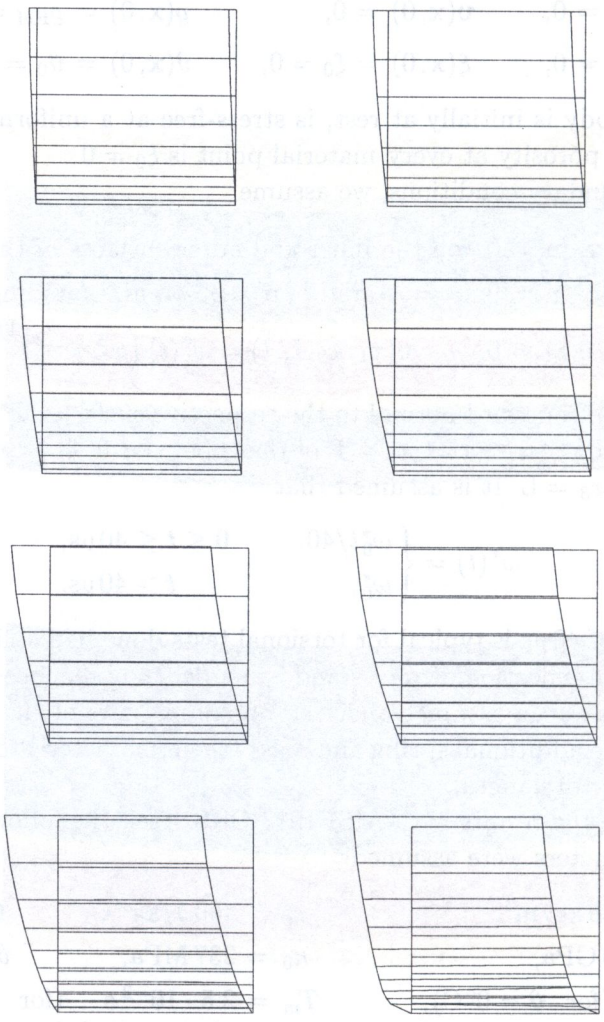

FIG. 7. Evolution of the deformation of the mesh for the segment for 2-D model.

beginning of the process ($t = 40\,\text{ms}$), the deformation confirms the well-known linear changes of twisting angle while at the end ($t = 320\,\text{ms}$), high gradients of deformations concentrate around the center of the tube.

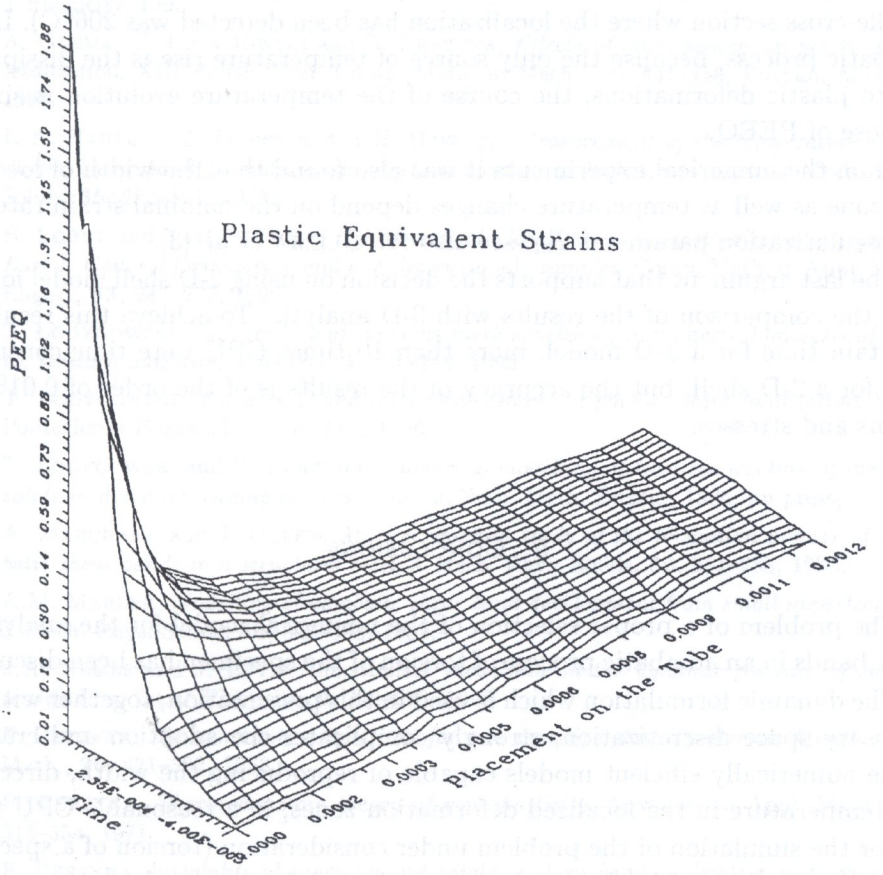

FIG. 8. Evolution of the plastic equivalent strain distribution.

The important results illustrating the evolution of plastic deformation of a typical segment as a function of the position on the segment and the time of the process are summarized in Fig. 8. On the vertical axis the equivalent plastic strains PEEQ are presented, when on the left-hand side horizontal axis we have process time, and on right-hand side axis the tube height. PEEQ finally reach the value of about 180% and the width of shear band is of the order of $0.0002 - 0.0003\,\text{m}$, what is in a good agreement with the experimental results. Of course, using visco-plastic formulation one can not expect the sharp contours of the localization zones. Its diffusion depends on the constitutive parameters, in particular T_m – relaxation time of mechanical disturbances. In the case un-

der consideration, the width is estimated by the high gradients of deformations shown in Fig. 8. Similarly we have achieved a good agreement of numerical results with experiments when comparing the changes of temperature which, for the assumed $\eta = 0.9$, were about 180°C (in the experiment, maximum in the middle-cross section where the localization has been detected was 206°C). In the adiabatic process, because the only source of temperature rise is the dissipation due to plastic deformations, the course of the temperature evolution is similar to those of PEEQ.

From the numerical experiments it was also found that the width of localization zone as well as temperature changes depend on the nominal strain rate and the regularization parameter T_m; see also A. GLEMA *et al.* [3].

The last argument that supports the decision on using 2-D shell model follows from the comparison of the results with 3-D analysis. To achieve this result for a certain time for a 3-D model, more than 10 times CPU were time-consumed than for a 2-D shell, but the accuracy of the results is of the order of 0.01% for strains and stresses.

5. CONCLUSIONS

The problem of a proper selection of the numerical model for the analysis of shear bands in an adiabatic process of torsion of the specimen has been discussed.

The dynamic formulation which is used in this presentation, together with the necessary space discretization, strongly complicates the adoption and creation of the numerically efficient models capable of reproducing the width, directions and temperature in the localized deformation zones, in a reasonable CPU time.

For the simulation of the problem under consideration (torsion of a specimen in a split Hopkinson bar), the chosen shell model seems to be adequate and reproduces the results of the known laboratory tests with a good accuracy.

The modelling of some of the specimens (thin-walled tubes) requires a proper definition of additional structural elements (concentrated mass and spring) which allows for a more precise formulation of the boundary and initial conditions.

ACKNOWLEDGMENT

The paper has been prepared within the research programme sponsored by the Committee of Scientific Research under Grant 7-T07-A013-10. Some computations were performed in Poznan Supercomputing and Networking Center.

REFERENCES

1. ABAQUS 5.6 *Manuals*, Hibbitt, Karlsson & Sorensen Inc., 1996.
2. R.C. BATRA and X. ZHANG, *On the propagation of a shear band in a steel tube*, Int. J. Plasticity, 1993.
3. A. GLEMA, T. ŁODYGOWSKI and P. PERZYNA, *Effects of microdamage in plastic strain localization*, XIII Polish Conf. Comp. Meth. in Mech., pp. 451–458, Poznań, May 5-8, 1997.
4. K.A. HARTLEY, J. DUFFY and R.H. HAWLEY, *Measurement of the temperature profile during shear band formulation in steels deforming at high strain rates*, J. Mech. Phys. Solids, **35**, 283–301, 1987.
5. B. LORET and J.H. PREVOST, *Dynamic strain localization in elasto-visco-plastic solids. Part 1. General formulation and one-dimensional examples*, Comp. Meth. in Appl. Mech. Engng., **83**, 247–273, 1990.
6. T. ŁODYGOWSKI, *On avoiding of spurious mesh sensitivity in numerical analysis of plastic strain localization*, CAMES, **2**, 231–248, 1995.
7. T. ŁODYGOWSKI, *Theoretical and numerical aspects of plastic strain localization*, Wyd. Politechniki Poznańskiej, No. **312**, 1996.
8. T. ŁODYGOWSKI and P. PERZYNA, *Numerical modelling of localized fracture of inelastic solids in dynamic loading processes*, Int. J. Num. Meth. Engng., 1996, [in press].
9. A. MARCHAND and J. DUFFY, *An experimental study of the formation process of adiabatic shear bands in a structural steel*, J. Mech. Phys. Solids, **36**, 251–283, 1988.
10. A.M. MERZER, *Modelling of adiabatic shear band development from small imperfections*, J. Mech. Phys. Solids, **30**, 323–338, 1982.
11. J.A. NEMES and J. EFTIS, *Constitutive modelling on the dynamic fracture of smooth tensile bars*, Int. J. Plasticity, **9**, 243–270, 1993.
12. P. PERZYNA, *The constitutive equations for rate sensitive plastic materials*, Quart. Appl. Math., **20**, 321–332, 1963.
13. P. PERZYNA, *Thermodynamic theory of viscoplasticity*, Advances in Appl. Mech., **11**, 313–354, 1971.
14. P. PERZYNA, *Instability phenomena and adiabatic shear band localization in thermoplastic flow processes*, Acta Mech., **106**, 173–205, 1994.
15. H.M. ZBIB and J.S. JURBAN, *Dynamic shear banding: A three-dimensional analysis*, Int. J. Plasticity, **8**, 619–641, 1992.

LABORATORY FOR COMPUTER METHODS IN ENGINEERING,
INSTITUTE OF STRUCTURAL ENGINEERING,
POZNAŃ UNIVERSITY OF TECHNOLOGY.

e-mail: glema@put.poznan.pl
kakol@put.poznan.pl
lodygowski@put.poznan.pl

Received November 14, 1997.